Available online at www.sciencedirect.com
ScienceDirect
Biochemical and Biophysical Research Communications 359 (2007) 1–7
BBRC
www.elsevier.com/locate/ybbrc

Three-dimensional nanometry of vesicle transport in living cells using dual-focus imaging optics

Tomonobu M. Watanabe [a,1], Takashi Sato [b], Kohsuke Gonda [a], Hideo Higuchi [a,*]

[a] *Biomedical and Engineering Research Organization, Tohoku University, Sendai, Miyagi 980-8579, Japan*
[b] *Department of Materials Science, Graduate School of Engineering, Tohoku University, Sendai, Miyagi 980-8579, Japan*

Received 11 April 2007
Available online 4 May 2007

Abstract

Dual-focus imaging optics for three-dimensional tracking of individual quantum dots has been developed to study the molecular mechanisms of motor proteins in cells. The new system has a high spatial and temporal precision, 2 nm in the x–y sample plane and 5 nm along the z-axis at a frame time of 2 ms. Three-dimensional positions of the vesicles labeled with quantum dots were detected in living cells. Vesicles were transported on the microtubules using 8-nm steps towards the nucleus. The steps had fluctuation of ~20 nm which were perpendicular to the axis of the microtubule but with the constant distance from the microtubule. The most of perpendicular movement was not synchronized with the 8-nm steps, indicating that dynein moved on microtubules without changing the protofilaments. When the vesicles changed their direction of movement toward the cell membrane, they moved perpendicular with the constant distance from the microtubule. The present method is powerful tool to investigate three dimensional movement of molecules in cells with nanometer and millisecond accuracy.

Keywords: Nanotechnology; Step size; Dynein; 3D; Kinesin

Motor proteins such as dynein, kinesin, and myosin play roles in cell motility such as vesicle transport, mitosis, and muscle contraction [1,2]. To describe the mechanisms of motility at a molecular level, single molecule studies including *in vitro* motility assay have been used [3–7]. Despite all the *in vitro* measurements performed using purified motor proteins in artificial solutions, it is important to investigate the motility of these proteins in living cells because physiological conditions in the cell environment are very different to those in *in vitro* assays [8–10].

In living cells, cytoplasmic dynein transports vesicles bound to its tail domain via membrane associated proteins [1]. The single particle imaging and tracking techniques using fluorescence dyes such as GFP or quantum dots observed the behavior of the vesicles in cells with nanometer and millisecond accuracies [7,9]. Dynein and kinesin transport vesicles with successive 8 nm steps in living cells [11–13] which is the same as that *in vitro* [7,14]. Many questions, however, have arisen about the *in vivo* behaviors of the motor proteins. Is dynein responsible for switching the protofilaments? Is the vesicle transport obstructed by the cytoskeletal network [1,2]? Since the motor proteins are arranged and work three-dimensionally (3D) in cells, it was difficult to answer these questions from results obtained by measurements of the movements viewed in two dimensions under a conventional microscope.

In the previous works, 3D tracking of particle movements has been constructed by moving the focal position by changing the position of an objective [15–17]. However, the method is not suitable for tracking fast biological pro-

* Corresponding author. Fax: +81 22 217 5753.
E-mail address: higuchi@tubero.tohoku.ac.jp (H. Higuchi).
[1] Present address: PREST, Japan Science and Technology Agency, Kawaguchi, Saitama, Japan.

0006-291X/$ - see front matter © 2007 Elsevier Inc. All rights reserved.
doi:10.1016/j.bbrc.2007.04.168

cesses that occur in a millisecond time scale because of the limitations of the speed of moving the objective. To overcome this problem, we developed a new optical method of dual view optics, which allows us to visualize three-dimensional biological processes with high temporal (2 ms) and spatial (2–5 nm) precisions without moving the objective. Using this technique we observed the inward transport of the membrane protein labeled with quantum dots (QDs) presumably by dynein in living cells.

Materials and methods

DIO (dual-focus imaging optics) system. The optical system for DIO consisted of an epi-fluorescent microscope (IX-71, Olympus), an EM camera (Ixon DV860, Andor), and a Piezo actuator having a electrostatic sensor (FB010-C, Nanocontrol). An area $\sim 10 \times 10\ \mu m^2$ was illuminated by a green laser (532 nm, 0.1 mW/μm^2 for each specimen, Big Sky laser) using diagonal irradiation [13]. The fluorescence of the quantum dots was filtered using a high-pass filter (transmission wavelength >580 nm; Omega). The Piezo actuator moved the position of the objective by the Piezo driver having a positional feedback loop (NC1100, Nanocontrol). We analyzed the data in which root-mean-square noise was <10 nm.

Preparation of anti-HER2-QDs and cells. HER2 (human epidermal growth factor receptor 2) on the membrane was labeled with multiple quantum dots via an anti-HER2 antibody according to the method reported previously [13]. Human breast cancer cells, KPL-4 cells, were cultured on a coverslip in DMEM (Gibco) containing 5% FBS (fetal bovine serum, Gibco) at 37 °C in 5% CO_2. Just prior to the experiment, FBS was removed for an hour to starve the cells, and the quantum dot-anti-HER2 antibodies were added to the cells [13]. To observe steps clearly, the experiments of 3D imaging were performed at low temperature 16–18 °C under the epi-fluorescence microscope with DIO system [13].

Results and discussion

DIO (dual-focus imaging optics) system and 3D single particle tracking

In order to track the 3D movement of single fluorescent particles, we developed a new optical system that two separated images at distinct focal positions were taken with an EM-CCD camera, called DIO (Fig. 1A). A narrow image of a sample on an epi-fluorescence microscope went through a slit positioned at the imaging surface ("Slit" in Fig. 1A). The optical pathway was split into two pathways by a half mirror (HM in Fig. 1A). Moving either L3 or L4 along the optical axis produced a difference between the two pathlengths. The difference in the optical lengths resulted in the difference in the focuses and magnification of the two images on the camera (an inset image in Fig. 1A). The distance between the two focal positions was set to ~1 μm in the present study and the ratio of magnification of the two pathways was ~0.96 (Supplement 1). The two images of a quantum dot were fitted to 2D Gaussian functions [13]. The difference in the fluorescence intensities at the centroid of the functions fit to was plotted as the function of z-position of the quantum dots (Fig. 1C). This curve was taken before every experiment as a calibration curve (Fig. 1C). The x–y position of a quantum dot was determined by fitting the images with 2D Gaussian functions as previously reported [6,7,9,13]. The spatial resolution was highly dependent on the number of photons emitted from a fluorophore [18]. Quantum dots were used in this study because of their superior fluorescence durabil-

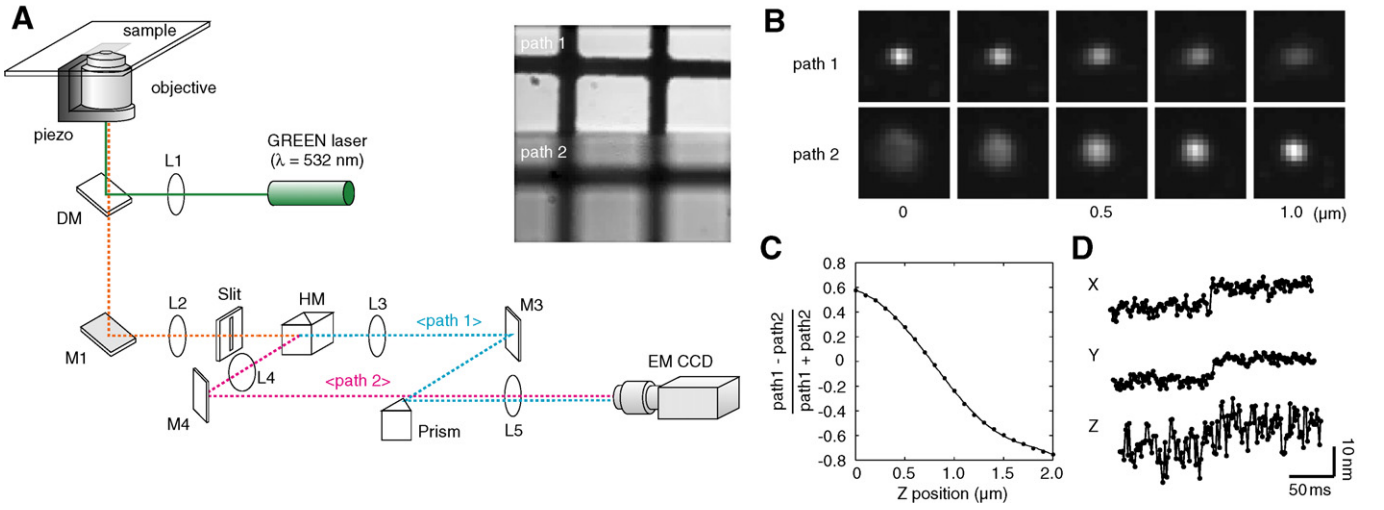

Fig. 1. Three-dimensional single particle tracking. (A) Schematic drawing of an optical set up for dual-focus imaging (DIO). A Piezo actuator bound to the objective. L, lens; M, mirror; DM, dichroic mirror; HM, half mirror cube. An inset panel shows an image of a test pattern of a square lattice (10 μm). Upper image is an image just in focus. (B) Fluorescent images at two distinct focus positions (path 1 and path 2). Quantum dot is located between the two focusing positions. An objective was moved along the optical axis (z-axis). (C) Calibration curve of z-position vs difference of the fluorescent intensities. The fluorescent intensities were recorded as the quantum dots moved along the z-axis. The division of the difference between the intensities in the two pathways and the addition of them was represented as (path 1 − path 2)/(path 1 + path 2). When quantum dots were moved in cells, z-position in the calibration curve was multiplied by the refractive index ratio, 0.88, of water, 1.33 to oil, 1.52. (D) Accuracy of the present methods. Quantum dot(s) fixed on a coverslip were moved by 10 nm steps using a Piezo actuator. The position of the Quantum dot(s) was determined with a temporal resolution of 2 ms with noise of 2.0 nm (x-axis and y-axis) and 5.3 nm (z-axis).

ity [7,13,19,20]. The spatial precisions of the dots fixed on a coverslip using the 3D tracking system were 2.2, 1.5, and 5.3 nm on the x, y, and z directions, respectively, with time resolution of 2 ms (Fig. 1D).

3D vesicle transport in living cells

In order to observe 3D movements of vesicles in living cells, quantum dots coated with anti-HER2 antibodies (human epidermal growth factor receptor 2) were mixed with breast cancer cells, KLP-4, which overexpresses HER2 on the cell membrane. Microtubule-based transport of the vesicles labeled with quantum dots (QD-vesicles) in the cytosol were visualized using diagonal illumination (Fig. 2A) [13]. The QD-vesicles moved in one direction i.e. towards the nucleus (Fig. 2B and Movie S1), and occasionally moved away from the nucleus to the cell membrane. The fluorescence intensity in dual images changed with time (Fig. 2B); for example, intensities on the left panels in Fig. 2B were low at 0 and 3 s and high at 1.2 s. These indicate the movement of z direction. QD-vesicles moved on GFP-microtubules as observed by confocal microscopy (Movie S2), confirming that the vesicles were indeed transported by a microtubule-based motor, either dynein or kinesin. Movements of QD-vesicles presumably by dynein from the cell membrane to the peri-nuclear region were also recorded. The moving QD-vesicles transported in 3D space were successfully monitored for a precision of a few nanometers on xy-plane and several nm on z-axis with 2 ms resolution using the DIO system (Fig. 2C and D).

How does dynein walk on a microtubule three-dimensionally with nanometer accuracy while transporting a vesicle? Smooth traces of the displacements were produced by averaging 100 points over a 200 ms period to follow the overall pathways of the QD-vesicles roughly. All of the smooth traces ($n = 57$) were then fitted approximately to the planes. Thirty-eight traces (67%) could be well fitted to a single plane with the standard deviation of the distance between the traces and the fitted plane being <10 nm (mean = 4.6 nm) (Fig. 3A). If artificial random traces were fitted to a plane (Supplement 2A), the standard deviation of the distance was not less than 10 nm ($n = 100$, Supplement 2B). Thus, the planar movements were not part of the random movements. Twelve traces (21%) could not be fitted by a single plane, but were well fitted to two or

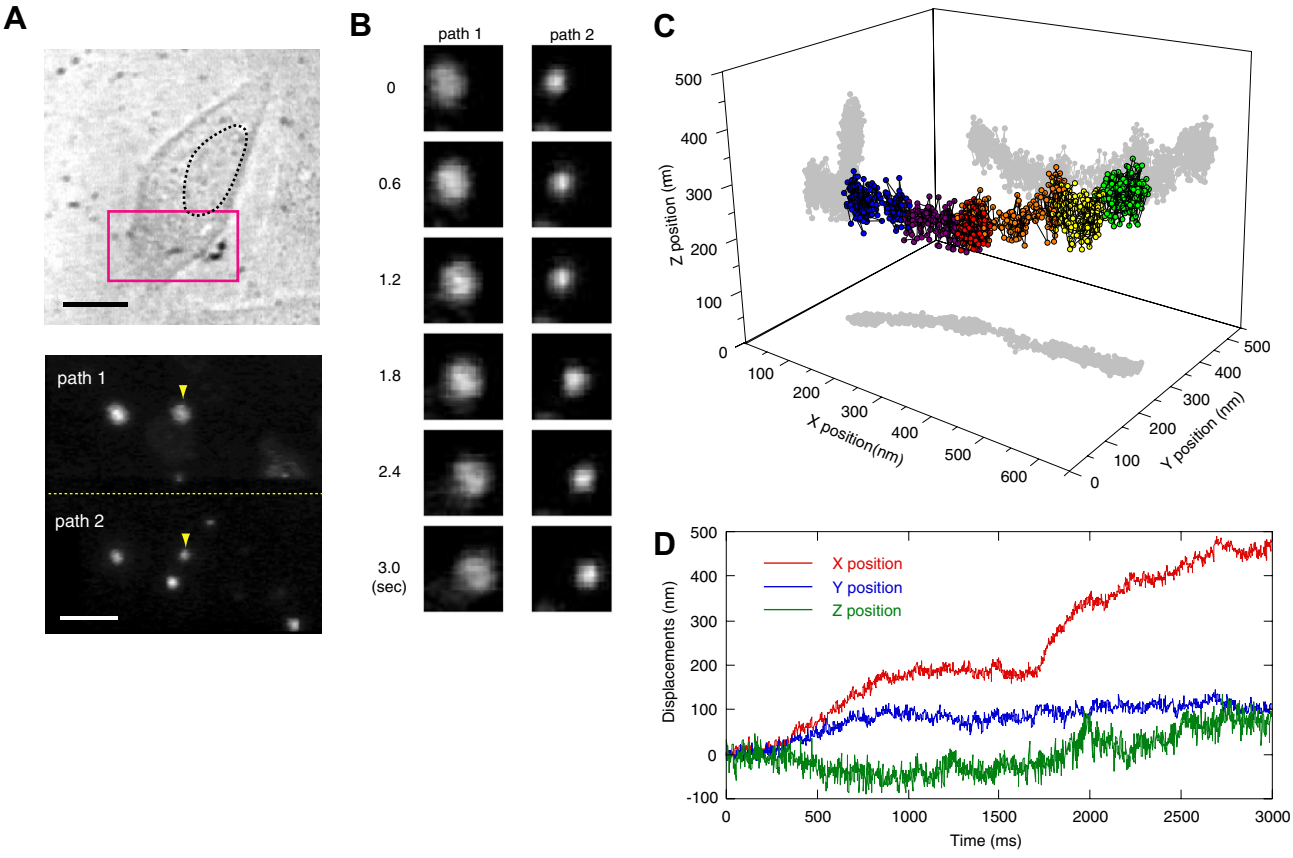

Fig. 2. Three-dimensional tracking of a moving vesicle in a living cell. (A) A bright field image (upper) and fluorescence images (lower) obtained using DIO. The red rectangle indicates the fluorescent imaging area. The fluorescent images of vesicles labeled with quantum dots were in the cell at two distinct focus positions. Yellow arrowheads indicate the vesicle being transported towards the nucleus. Calibration bars were 10 μm in a upper panel and 5 μm in a lower one. (B) Time course of the fluorescent images of the moving vesicle indicated by the yellow arrowheads in (A). The vesicle moved to the right, which is the direction towards the peri-nuclear region. (C) 3D movements of the transport of the QD-vesicle towards the peri-nuclear region. Six colors from blue to green indicate the running time from 0 to 3 s (0.5 s each color). (D) The time courses of x (red), y (blue), and z-positions (green) in (C).

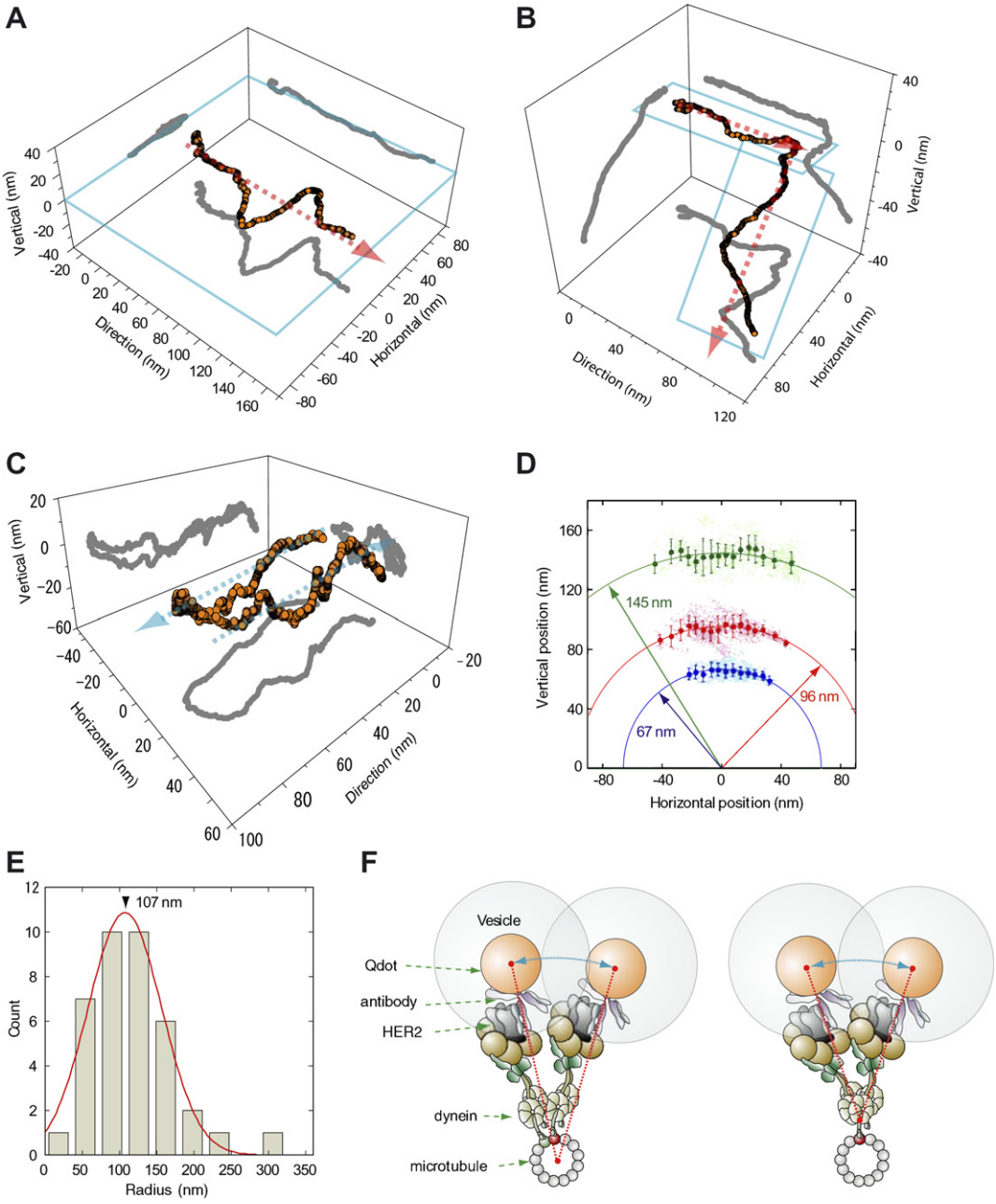

Fig. 3. Movement of the vesicle transport by dynein in living cells. (A) Typical traces of the movements in the different planes. The traces were well fitted with a primary plane surface ($f(x,y,z) = ax + by + cz + d$; a, b, c, and d are the fitting parameters (cyan line). (B) Typical trace when QD-vesicle transfers from one microtubule to another microtubule. The trace was fitted well to two planes. Cyan lines indicate the data have been fitted by two planes. (C) A typical trace of the directional switching by most likely dynein and kinesin. (D) Vertical–horizontal plots of the 3D traces. The graph shows the typical three traces (red, blue, and green). Plots and bars indicate the average values taken every 5 nm along the horizontal axis and the standard deviations, respectively. Traces were fitted with a circle. Cyan arrows in (A), (B), and (C) indicate the direction of movement of the vesicles. (E) Histogram of the radius of the cylindrical surfaces. The distribution followed to a Gaussian distribution with a peak of 107 ± 49 nm (red line, $n = 38$). (F) Possible models to explain the cylindrical movements of the vesicle during transportation. The left panel shows the model where dynein transfers from one protofilament to another on a microtubule. The right panel shows the model that dynein did not transfer but fluctuate around the binding site of dynein and tubulin.

three planes with standard deviations <10 nm (Fig. 3B). The remaining seven traces could not be distinguished from random movement because of the large standard deviations (>10 nm). Helical type movements were not observed in any of the traces.

An abrupt change in the direction of movement of the vesicles was observed in three traces (5%) which are fitted to one plane. In all cases, the QD-vesicles moved by 30–50 nm in the horizontal direction in a stepwise fashion when the direction of movement suddenly changed to the opposite direction (Fig. 3C and Fig. 3S). Kinesin is a motor that moves vesicles to the plus-end of a microtubule and is thought to be involved in this process by directly competing with dynein [12].

Three-dimensional nanometry of vesicle transport

To examine the systematic displacement of quantum dots from the planes, the vertical position displaced from the plane and horizontal positions perpendicular to moving direction were repotted (Fig. 3D). These plots could be well fitted to arcs, a part of a circle. The mean radius of the arcs was determined to be 107 nm (Fig. 3E). The arcs indicate the distance between the center of a microtubule and the center of quantum dots because the distance, 107 nm, is consistence with the distance estimated from the radius of a microtubule (13 nm), the length of the dynein (50–80 nm), the length of the membrane protein and antibody complex (10–20 nm) and the radius of a quantum dot (~12 nm) (Fig. 3F) [21,22]. The approximately planar or exactly arc movements suggest that vesicles were transported on single microtubules. The traces which fitted to two or three planes suggest that vesicles can switch from one microtubule to another during vesicle transport.

Movement in the horizontal axis (~20 nm in S.D.) was much larger than movement in the vertical axis (~4 nm) (Fig. 3D). There are two possibilities that could explain the large movements in the horizontal plane. One is that dynein steps onto the neighboring protofilaments (Fig. 3F, left) [22]. This is suggested from studies that recombinant yeast dynein was shown to step to neighboring protofilaments in the *in vitro* assays [14]. In this model, the horizontal movement should occur at steps in travel direction. The other possibility is that the flexible linker, stalk or tail, in dynein allows the quantum dot to fluctuate around the linker (Fig. 3F, right) [23–25]. In this model, the horizontal movement does not need to occur at the directional steps.

To distinguish between these two possibilities, the step sizes of the QD-vesicles in directional, horizontal, and vertical movements were analyzed (Fig. 4). Steps were detected in the directional and the horizontal orientation using our computing algorithm (Fig. 4A, red and blue lines) [13], while steps in the vertical orientation was within a few nanometers which is not distinguished from the noise. The histogram of the step sizes in the directional orientation showed three distinct Gaussian distributions with the main peak occurring at 8.1 nm and minor peaks at 16 and −8 nm (Fig. 4B). The histogram of the pairwise distances also confirmed that 8 nm steps occurred in the directional movement (Fig. 4C) [3]. The 8 nm unitary steps were

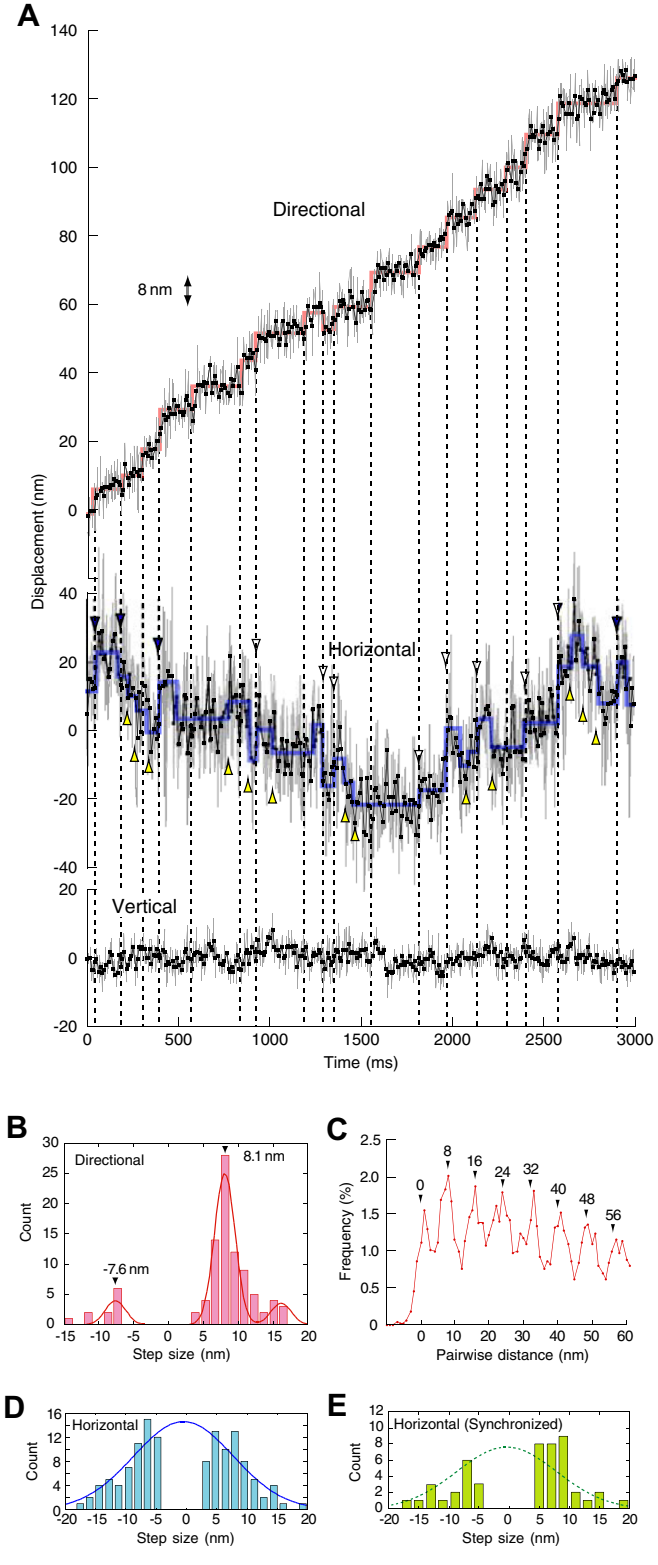

Fig. 4. Three-dimensional nanometry of a moving vesicle. (A) The typical time courses in the directional, horizontal, and vertical axes. Data points of the displacements were analyzed at 2 ms intervals (Gray lines). Five points were then averaged to smoothen the traces as shown by black squares and lines. A step size larger than 4 nm was detected here by the computer algorithm [13]. Broken lines indicate the moments where the 8 nm steps occured along the directional axis. Yellow arrowheads indicate the steps are not in synchronization with the directional 8 nm steps. (B) Histogram of the step size in the directional axis. The graph was fitted with multiple Gaussian functions. The peaks ± widths are 8.1 ± 1.5 nm at forward steps and −7.6 ± 1.4 nm at backward steps. (C) Histogram of the all pair wise distance analysis [3] (40 ms interval) of the trace in directional axis shown in (A). (D) Histogram of the step size in the horizontal axis. The graph was fitted with a Gaussian function with the peak of 0.5 nm and a width of 8.2 nm. (E) Histogram of the step size in the horizontal axis when horizontal steps were in synchronization with the directional 8 nm steps. Dotted line indicates the Gaussian curve the same as that in (D).

consistent with the value previously determined in two dimensions in living cells [7,11–14].

Some of horizontal steps synchronized with the directional 8 nm steps (Fig. 4A, blue arrowheads), but many of them did not (yellow arrowheads). The sizes of both synchronized and non-synchronized steps were fitted to a Gaussian distribution with the peak at 0.5 nm and a standard deviation of 8.2 nm (Fig. 4D and E). The horizontal step sizes of 8.2 nm were much smaller than ~50 nm which was estimated from the model that describes dynein changing the protofilaments during movement. These results suggest that dynein primarily moves on certain protofilaments in the microtubules with small fluctuation around the microtubule. In a living cell, there are many obstacles such as other vesicles, organelles, and the cytoskeletal meshwork that will prevent vesicle transport from moving in a straight line along a protofilament on a microtubule. Dynein may be able to subtly change the structure of the flexible linker to encounter obstacles (Fig. 3F, right).

The horizontal step size of 30–50 nm in Fig. 3C (Supplement 3) was comparable to the horizontal step size of ~50 nm predicted from Fig. 3F (left), suggesting that these two motors, presumably dynein and kinesin, move on distinct protofilaments or bound to a vesicle separatedly.

Here, we successfully observed vesicle transport in three dimensions in living cells with nanometer and millisecond accuracy using the DIO system. We found that dynein primarily walks in straight lines on a protofilament of a microtubule and changes protofilaments minor. The lateral displacement of QD-vesicles can be explained by the flexible linker region in the dynein molecule, and this would contribute to the robustness of the dynein-based vesicle transport through the cytoskeletal meshwork filled with organelles and other vesicles without having to switch to other protofilaments. The present method is powerful tool to investigate many kinds of 3D movement of molecules in cells with nanometer and millisecond accuracy.

Acknowledgments

We gratefully acknowledge J.M. West for critical reading this manuscript. This work was supported by Grants-in-Aid for Scientific research in Priority Areas from the Japan MEXT (H.H.), Special Coordination Funds for Promoting Science and Technology of JST (H.H., K.G. and T.M.W.) and CREST of JST (H.H.).

Appendix A. Supplementary data

Supplementary data associated with this article can be found, in the online version, at doi:10.1016/j.bbrc.2007.04.168.

References

[1] N. Hirokawa, Kinesin and dynein superfamily proteins and the mechanism of organelle transport, Science 279 (1998) 519–526.
[2] R.-I. Tuxworth, M.A. Titus, Unconventional myosins: anchors in the membrane traffic relay, Traffic 1 (2000) 11–18.
[3] K. Svoboda, C.-F. Schmidt, B.-J. Schnapp, S.-M. Block, Direct observation of kinesin stepping by optical trapping interferometry, Nature 365 (1993) 721–727.
[4] T. Funatsu, Y. Harada, M. Tokunaga, K. Saito, T. Yanagida, Imaging of single fluorescent molecules and individual ATP turnovers by single myosin molecules in aqueous solution, Nature 374 (1995) 555–559.
[5] A. Ishijima, H. Kojima, T. Funatsu, M. Tokunaga, H. Higuchi, H. Tanaka, T. Yanagida, Simultaneous observation of individual ATPase and mechanical events by a single myosin molecule during interaction with actin, Cell 92 (1998) 161–171.
[6] A. Yildiz, J.-N. Forkey, S.-A. McKinney, T. Ha, Y.-E. Goldman, P.-R. Selvin, Myosin V walks hand-over-hand: single fluorophore imaging with 1.5-nm localization, Science 300 (2003) 2061–2065.
[7] S. Toba, T.-M. Watanabe, L. Yamaguchi-Okimoto, Y.-Y. Toyoshima, H. Higuchi, Overlapping hand-over-hand mechanism of single molecular motility of cytoplasmic dynein, Proc. Natl. Acad. Sci. USA 103 (2006) 5741–5745.
[8] Y. Sako, J. Ichinose, M. Morimatsu, K. Ohta, T. Uyemura, Optical bioimaging: from living tissue to a single molecule: single-molecule visualization of cell signaling processes of epidermal growth factor receptor, J. Pharmacol. Sci. 93 (2003) 253–258.
[9] A. Yildiz, P.-R. Selvin, Fluorescence imaging with one nanometer accuracy: application to molecular motors, Acc. Chem. Res. 38 (2005) 574–582.
[10] Y. Chen, B.-C. Lagerholm, B. Yang, K. Jacobson, Methods to measure the lateral diffusion of membrane lipids and proteins, Methods 39 (2006) 147–153.
[11] C. Kural, H. Kim, S. Syed, G. Goshima, V.-I. Gelfand, P.-R. Selvin, Kinesin and dynein move a peroxisome in vivo: a tug-of-war or coordinated movement? Science 308 (2005) 1469–1472.
[12] X. Nan, P.-A. Sims, P. Chen, X.-S. Xie, Observation of individual microtubule motor steps in living cells with endocytosed quantum dots, J. Phys. Chem. B, Condens Matter Mater. Surf. Interfaces Biophys. 109 (2005) 24220–24224.
[13] M.-T. Watanabe, H. Higuchi, Stepwise movements in vesicle transport of HER2 by motor proteins in living cells, Biophys. J., 92 (2007) 4109–4120.
[14] S.L. Reck-Peterson, A. Yildiz, A.P. Carter, A. Gennerich, N. Zhang, R.D. Vale, Single-molecule analysis of dynein processivity and stepping behavior, Cell 28 (2006) 335–348.
[15] I.-M. Peters, Y. van Kooyk, S.-J. van Vliet, B.-G. de Grooth, C.-G. Figdor, J. Greve, 3D single-particle tracking and optical trap measurements on adhesion proteins, Cytometry 36 (1999) 189–194.
[16] V. Levi, Q. Ruan, E. Gratton, Melanosomes transported by myosin-V in Xenopus melanophores perform slow 35 nm steps, Biophys. J. 88 (2005) 2919–2928.
[17] T. Ragan, H. Huang, P. So, E. Gratton, 3D particle tracking on a two-photon microscope, J. Fluoresc. 16 (2006) 325–336.
[18] R.-E. Thompson, D.-R. Larson, W.-W. Webb, Precise nanometer localization analysis for individual fluorescent probes, Biophys. J. 82 (2002) 2775–2783.
[19] A.-P. Alivisatos, Semiconductor clusters, nanocrystals, and quantum dots, Science 271 (1996) 933–937.
[20] X. Michalet, F.-F. Pinaud, L.-A. Bentolila, J.-M. Tsay, S. Doose, J.-J. Li, G. Sundaresan, A.-M. Wu, S.-S. Gambhir, S. Weiss, Quantum dots for live cells, in vivo imaging, and diagnostics, Science 307 (2005) 538–544.
[21] O.-I. Wagner, J. Ascano, M. Tokito, J.-F. Leterrier, P.-A. Janmey, E.-L. Holzbaur, The interaction of neurofilaments with the microtubule motor cytoplasmic dynein, Mol. Biol. Cell 15 (2004) 5092–5100.

[22] H.S. Cho, K. Mason, K.X. Ramyar, A.M. Stanley, S.B. Gabelli, D.W. Denney Jr., D.J. Leahy, Structure of the extracellular region of HER2 alone and in complex with the Herceptin Fab, Nature 13 (2003) 756–760.
[23] X. Meng, M. Samso, M.-P. Koonce, A flexible linkage between the dynein motor and its cargo, J. Mol. Biol. 357 (2006) 701–706.
[24] S.-A. Burgess, M.-L. Walker, H. Sakakibara, K. Oiwa, P.-J. Knight, The structure of dynein-c by negative stain electron microscopy, J. Struct. Biol. 146 (2004) 205–216.
[25] M. Samso, M. Radermacher, J. Frank, M.-P. Koonce, Structural characterization of a dynein motor domain, J. Mol. Biol. 276 (1998) 927–937.